

UDC 620.92

**AUTONOMOUS WIND POWER SYSTEM OF HOUSEHOLD
ELECTRIC SUPPLY**

Halko Serhii

candidate of technical sciences, associate professor,
director of Educational-Scientific Institute General-University Preparation

Zharkov Anton

engineer

Dmytro Motornyi Tavria State Agrotechnological University

c. Melitopol, Ukraine

Abstract. The functional scheme of the power supply system of households based on a wind power plant of low power with an electric generator with excitation from constant neodymium magnets is provided, which provides a given voltage level at the consumer in non-stationary stochastic dynamic modes characterized by random wind speed and loading magnitude. A mathematical modeling of operating modes is performed and an adequate mathematical model describing stationary and transient processes in the proposed system is obtained.

Keywords: renewable energy sources, wind energy, wind power generation, energy conversion, energy storage batteries, voltage control

Introduction. Wind power is one of the fastest growing renewable energy sources in the last decade, providing about 3% of world electricity consumption [1,3]. The specificity of small households is due to relatively small electricity consumption and requires large-scale development of small wind power engineering, which, based on technical conditions, is limited to 10 kW. Market research on the market for wind energy equipment shows that small consumers intend to use wind turbines to meet their needs (for example, as power supplies for industrial and household equipment, lighting, charging of automotive battery, etc.). [4].

Wind power installation (WPI) converts the kinetic energy of the wind into an electric. Stand-alone WPI produce electricity for domestic and industrial needs and in modern terms, represent an alternative to traditional electricity supply [5].

The main element WPI there is a wind wheel (WW), which is characterized by the speed of the speed. Possibilities of increasing the speed of rotation WW limiting aerodynamic factors. Use for this purpose of reducers and other mechanical devices is inappropriate in terms of the appearance of additional energy losses and deterioration of the overall dimensions. In low-power plants most commonly used multipole generators on permanent magnets [5-7]. Perspective for this purpose are generators on permanent magnets, which are simple in design, reliable, do not require additional power of the winding of excitation [6,7].

The main feature of WPI there is a need to work in conditions of variable wind speed, the individual impulses of which can significantly exceed its average speed, and at other times the speed can drop significantly. This circumstance forces us to use in WPI complex mechanical or hydraulic speed control devices, and accordingly - output voltage generator, which essentially complicates and raises the whole structure and is unacceptable for the autonomous one WPI low power [8-10]. It is better to use installations with an intermediate link of a direct current and a buffer energy storage with the subsequent transformation of it into the voltage and the current of the industrial frequency [5]. In [11] it is recommended, based on the comparable characteristics of the generator and wind-wheel capacities, to adjust the power of the plant in the generator excitation circuit, which is unacceptable for the developed and patented non-direct-current wind turbine generators on permanent magnets [6,7].

Among the various types of energy storage devices, the most attractive means for a buffer energy storage in low power plants are accumulators [12], which at a sufficient wind speed are recharged, and when the wind speed falls and power shortages give energy to the load. For operative regulation of power from generator to load it is expedient to apply a resistive ballast load, which perceives excess power at high wind speeds [11].

In modern literature sufficiently developed typical circuits WPI large and medium power, as well as modes of operation of the generator with electromagnetic excitation or excitation from permanent magnets [5]. To a lesser extent, non-stationary dynamic regimes have been investigated WPI low power, characterized by the random wind speed and the random value of the load resistance provided the voltage is stabilized at the instantaneous values of the wind speed and the output voltage of the generator.

The aim of this study is development of the functional scheme of the power supply system on the basis of WPI low power generator with permanent magnets and simulation of its operation in conditions of random wind speed and random variation of load resistance change.

Experimental. Functional scheme of the proposed power supply system with WPI low power on an electric generator with permanent neodymium magnets is depicted in Fig. 1. The scheme works in the following way. Phase voltage from the generator G fed to a bridge unmanaged rectifier VD and throughdamping filter F enters the team bus B. It also connects a resistive ballast load BL and a rechargeable battery RB through the controller C «charge-discharge» of a battery. From the combined bus B the voltage goes to the inverterI, the output of which is on the load L tension is removed 220 V industrial frequency.

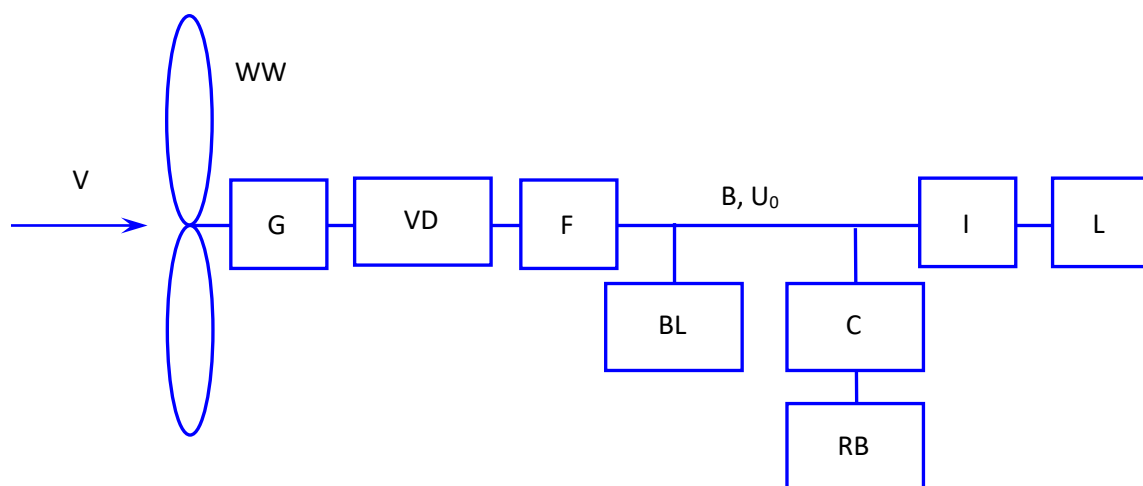


Fig. 1 Functional scheme of the power supply system on the basis of WPI

With an excess of generator power, which is expressed in an increase in voltage, due to an increase in wind speed V , the conductivity of the ballast load BL increases, which leads to the selection of excessive power. In addition, in these conditions there is the possibility of recharging the rechargeable battery RB ; her controller C provides charging current limitation and its full termination at maximum charge. As a result, the voltage on the combined bus B does not increase substantially. A similar work happens when the power consumed by the load decreases L . With complete loss of load power L and fully charged battery RB wind wheel WW discharged from the wind or braked, for example, the systems that are listed in [13,14]. Thus, the proposed system does not provide for mechanical control of the speed of the wind wheel WW ; this is done by adjusting the load of the generator G .

Power shortages occur when the wind speed is shorter V or on a load L on the inverter I . With a deficiency of power on the combined bus B conductance BL down to zero, and the battery pack RB , which is discharged, maintains voltage at a constant level. Controller C limits the discharge current of the rechargeable battery RB and stops it with its maximum allowable discharge. Change in the conductivity of the ballast load BL provided by connecting to the combined bus B low resistors through the frequency pulse width modulation device 4-6 kHz.

Results and discussion. A mathematical description of the operating modes of a generator with permanent magnets under the condition of a sinusoidal curve of the output voltage and of the unsaturated magnetic circuit is performed in orthogonal, q - coordinates with a forward rotation of the longitudinal axis. In such generators there are no special damping windings on the rotor; their role is played by massive parts of the rotor. According to research results [8], damping currents relatively little influence the mode of such a generator, so they are not considered further in the mathematical model. In addition, the change in the magnetic flux due to partial demagnetization is manifested only with currents close to the short circuit. Therefore, we further believe that the magnetic flux of magnets remains constant. It should be noted that such an assumption was made by the developers of the model of a machine with permanent magnets in the package of imitation modeling MATLAB Simulink.

Thus, the equation for the longitudinal and transverse component of the currents and voltage of the generator have the form [8]:

$$\begin{cases} 1,5ri_d + 1,5L_d \frac{di_d}{dt} + 1,5L_q i_q \Omega p + u_d = 0; \\ 1,5ri_q + 1,5L_q \frac{di_q}{dt} - 1,5L_d i_d \Omega p - 1,5\Psi \Omega p + u_q = 0, \end{cases} \quad (1)$$

where i_d , u_d , i_q , u_q - longitudinal and transverse components of phase voltages and currents at the output of the generator;

L_d , L_q - inductance of the phase winding of the generator stator along the corresponding axes;

p – the number of pairs of poles;

r - active resistance of the stator winding phase;

Ψ - flow grapping along the longitudinal axis of the generator.

Neglecting the electric inertia of the windings of the generator in comparison with its mechanical inertia and considering the generalized load impedance R_L mainly resistive, we obtain the last equation in the form

$$\begin{cases} 1,5ri_d + 1,5L_q i_q \Omega p + \frac{1}{\sqrt{3}} R_L i_d = 0; \\ 1,5ri_q - 1,5L_d i_d \Omega p - 1,5\Psi \Omega p + \frac{1}{\sqrt{3}} R_L i_q = 0, \end{cases} \quad (2)$$

where

$$i_q = \frac{1,5\Psi \Omega p \left(1,5r + \frac{1}{\sqrt{3}} R_L\right)}{L_d L_q (1,5\Omega p)^2 + \left(1,5r + \frac{1}{\sqrt{3}} R_L\right)^2} = \frac{1,5\Psi \Omega p L_d L_q}{1,5r + \frac{1}{\sqrt{3}} R_L}; \quad (3)$$

The equation of the dynamics of the mechanical part WPI has the form of equation of equilibrium of moments

$$\begin{aligned} J \frac{d\Omega}{dt} + k_{cf} \Omega + M_G &= M_{WW}; \\ M_G &= 1,5 p i_q [1,5\Psi + (L_d - L_q) i_d], \end{aligned} \quad (4)$$

where J - moment of inertia of rotating masses;

k_{cf} - coefficient of friction;

M_G - electromagnetic moment of the generator;

M_{WW} - torque winding torque, which depends on the speed of its rotation and wind speed [5]:

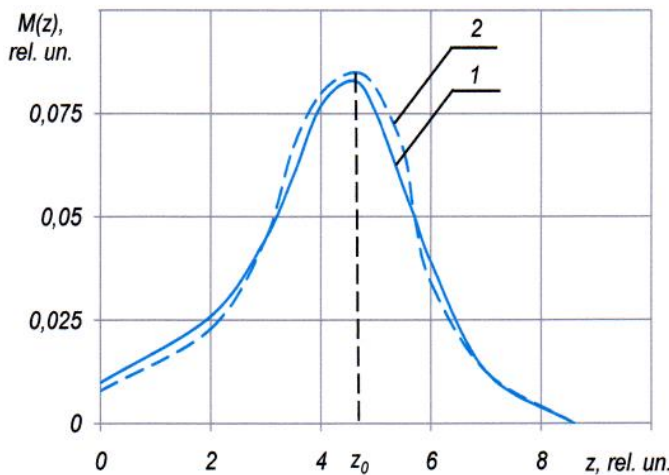
$$M_{WW} = M(z) \frac{D^3 \rho \pi V^3}{16}, \quad (5)$$

where D - diameter of the wind wheel;

ρ - air density;

$M(z)$ - relative moment of the wind wheel, which depends on the speed z .

A typical graph of the relative torque for a trilateral windrow, shown in Fig. 2 solid lines 1 [5].



1 – typical; 2 – approximated for (6)

Fig. 2 Dependencies of relative moment $M(z)$ from fast speed z

For modeling purposes, this moment is approximated by a nonlinear dependence

$$M(z) = k_1 e^{-k_2(z-z_0)^2} + k_3 e^{-k_4 z} + k_5 \sin z - k_6 z^5, \quad (6)$$

where $k_1 - k_6$ - coefficients of approximation.

In Fig. 2 approximated dependence (6) shown by dashed line 2 with parameter values:

$$k_1 = 0,09; k_2 = 0,35; k_3 = 0,006; k_4 = 0,03; k_5 = 0,009; k_6 = 3 \cdot 10^{-7}.$$

As it follows from Fig. 2, approximation sufficiently reflects the original curve, especially given that the original curve itself $M(z)$ usually presented in a very averaged form [5].

Graph of the dependence of ballast resistive load resistance r_{BL} from voltage u on the combined bus B depicted on Fig. 3, on which the given voltage is indicated $U_0=56$ B. At a voltage greater U_0 , resistance r_{BL} decreases, and the ballast load takes an excess of power, which stabilizes the tension on the combined bus B. With a lack of power, when the voltage decreases, ballast load resistance r_{BL} is increasing. Listed on Fig. 3 dependence $r_{BL} = f(u)$ at $u > U_0$ approximates the expression

$$r_{BL} = \frac{2}{u - U_0 + 0,002}, \quad (7)$$

where u – the current value of the voltage on the combined bus.

Partially linear approximation of the expression is also possible (7). When implementing the system, the law of high-frequency pulse-width modulation is constructed in such a way as to provide an average resistance value r_{BL} according to the curve (7).

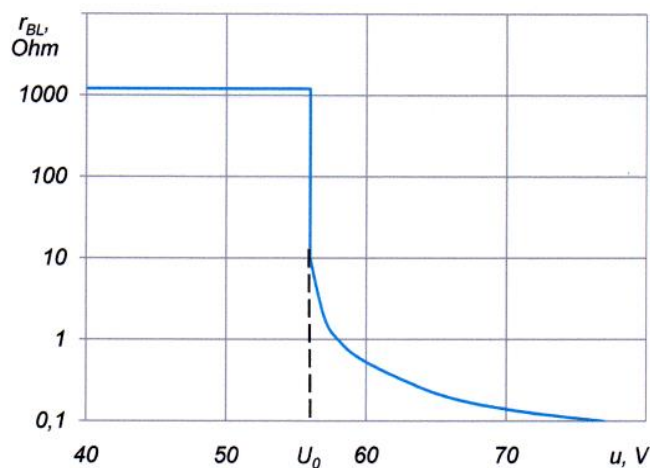


Fig. 3 Ballast load resistance r_{BL}

Idealized voltage-ampere characteristic (VAC) of rechargeable battery $I = f(u)$ depicted on Fig. 4 dashed line. Nearly the vertical portion of this curve at $I > 0$ matches charging mode, and with $I < 0$ - discharging mode. Horizontal areas are non-working and unacceptable; the battery controller precludes access to these areas, limiting the currents of charge and discharge almost to the vertical part of the characteristic.

Battery charge $g_{RB} = f(u)$ (at Fig. 4 - solid line), corresponding to this VAC, approximates the expression

$$\begin{cases} g_{RB}(u) = \frac{b_1}{u} - \frac{b_2}{U_0} e^{-b_2(u-U_0)}; u > U_0; \\ g_{RB}(u) = \frac{b_1}{u} - \frac{b_1}{U_0} e^{b_2(u-U_0)}; u < U_0, \end{cases} \quad (8)$$

where b_1, b_2 – coefficients of approximation.

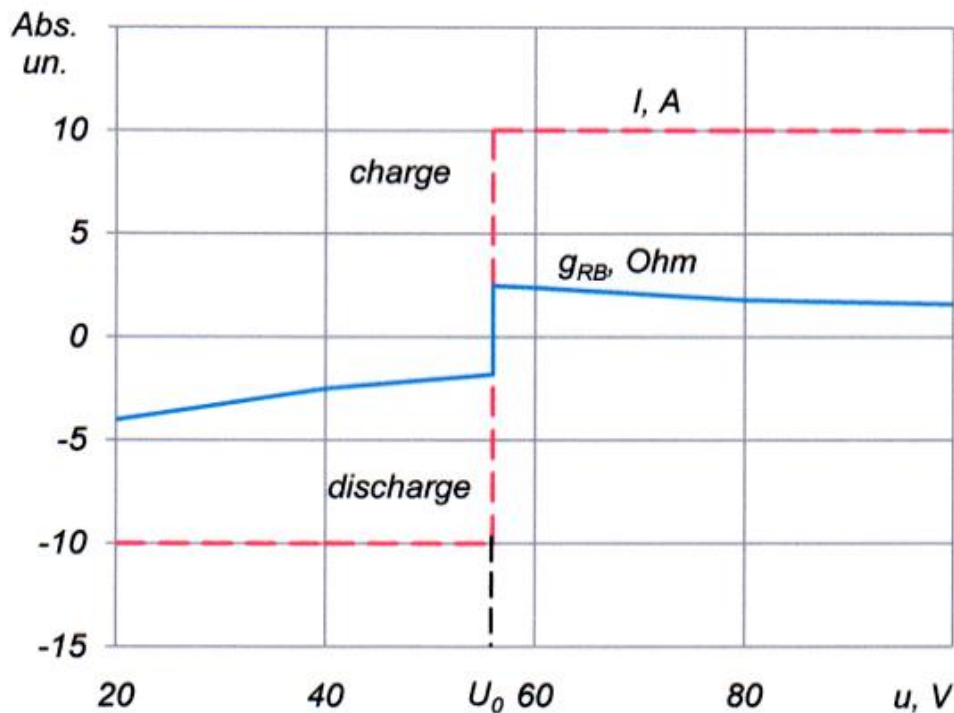


Fig. 4 Voltage-ampere characteristics of the battery

The first terms in these expressions represent horizontal sections VAC, but exponential - provide a smooth transition between these areas along the almost vertical line, which corresponds to the regimes “charge-discharge” of a battery. Coefficient $b_1 = 20$ determines the marginal current of the battery; coefficient $b_2 = 10$ defines the degree of smoothing of the corners of the characteristic and the level of inclination from the vertical of the working area “charge-discharge” of a battery (is selected experimentally). Thus, the generalized load resistance is determined by the equation:

$$R_L = R_L(t, u) = \left(\frac{1}{r_L(t)} + \frac{1}{r_{BL}(u)} + g_{RB}(u) \right)^{-1}, \quad (9)$$

where r_L - resistance of payload (input impedance of the inverter).

The simplified mathematical description of the “rectifier-filter” node has the form:

$$T_F \frac{du}{dt} + u = R_L I_L, \quad (10)$$

where T_F – constant time filter;

$$I_L = \sqrt{i_d^2 + i_q^2} \text{ - load current.}$$

Charge q the battery depends on its current and is described by the equation:

$$T_{RB} \frac{du}{dt} = u g_{RB}(u), \quad (11)$$

where T_{RB} – constant time characterizing the capacity of the battery, and hence the speed of its charge and discharge.

The right side of the equation (11) - battery current, limited from the top and bottom at discharge and charge, and is equal to zero: when the battery is discharged $u < U_0$; and when the battery is fully charged, and $u > U_0$.

So, equation (1) - (6) describe the mechanical dynamics WPI; equation (7) with (1), (7) - (9) describes the voltage u on the combined bus; equation (11) with (8) characterizes the current battery charge.

On Fig. 5 stationary schedules are presented WPI on an interval of 70 seconds at random wind speed $V(t)$, the value of which varied from 8,4 to 13,5 m/s, and the random nature of the change in load resistance $r_L(t)$ from 1,0 to 2,2 Ohm, which corresponds to the fluctuation of the load power P_L from 1,8 to 3,0 kW. The calculation is based on the mathematical model described above, for WPI with a generator for constant neodymium magnets, the design of which is patented by the authors of the work [7], with nominal power $P_{G.N} = 4$ kW, with the following numerical values of the parameters: inductance and phase resistance of the generator $L_d = 0,0032$ Gn, $L_q = 0,0027$ Gn, $r = 0,3$ Ohm; the number of pairs of poles $p = 16$; magnetic flux-grappling of permanent magnets to the pole $\Psi = 0,165$ Wb; coefficient of friction $k_{cf} = 0,01$; diameter of the wind wheel $D = 4,6$

m; moment of inertia of rotating masses $J = 11,1 \text{ kg}\cdot\text{m}^2$; time constants: $T_{VD} = 1,1 \text{ s}$, $T_{RB} = 20 \text{ s}$.

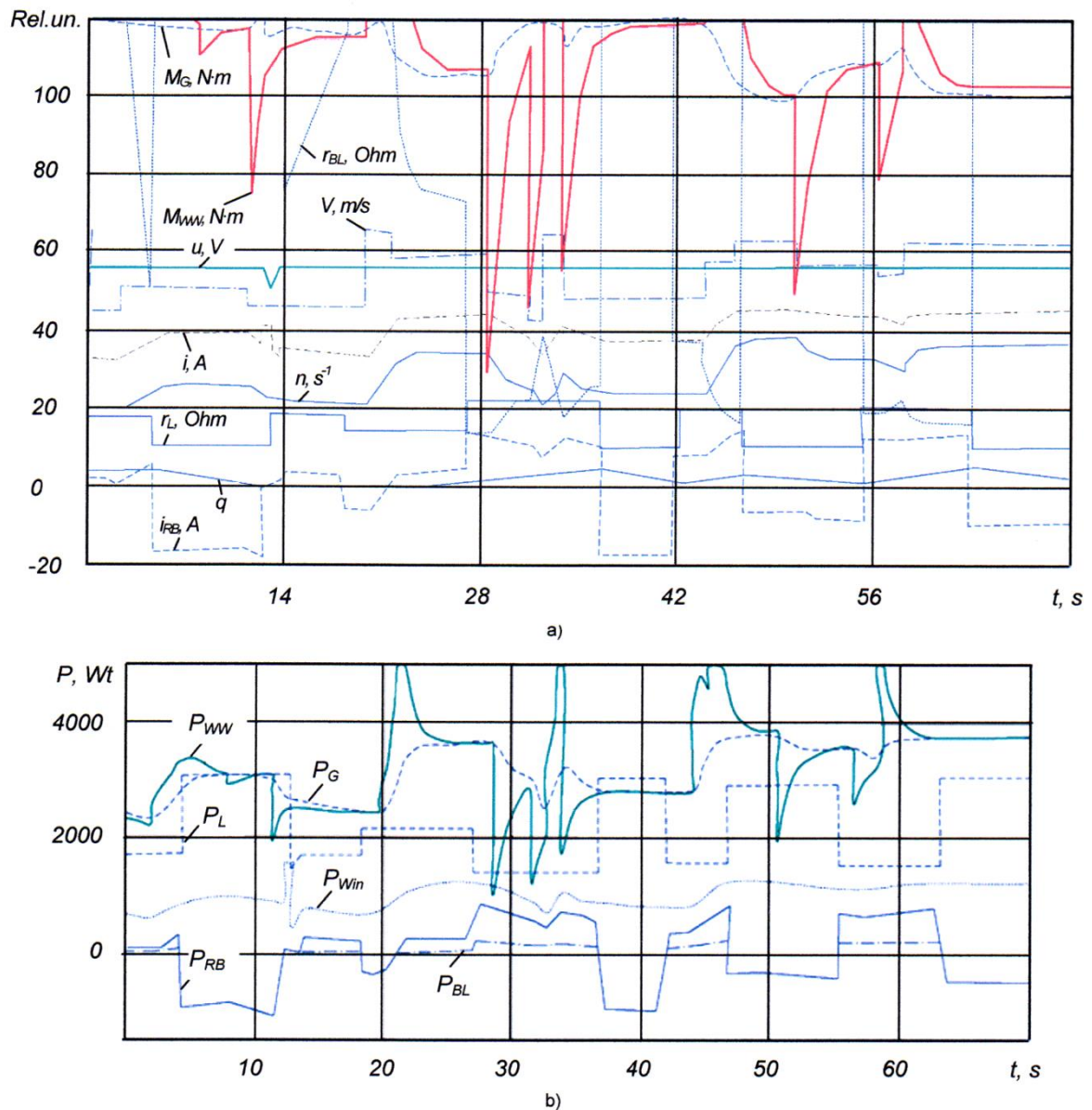


Fig. 5 Stationary mode of the wind power installation

On Fig. 5,a depicts the dependence of the basic parameters of the mode on time, and on Fig. 5,b - power. For clarity, the wind speed schedule is shown 5 times, and the load resistance graph $r_L(t)$ - increased by 10 times. Charts show, that WPI in general, successfully cope with the task of maintaining voltage u on the combined bus at the level 56 V. Small voltage deviations are only noticeable with significant differences

in load resistance and wind speed. So, the voltage drop across the bus was in the range of 12,3 to 14 V as a result of the adverse effect of reducing the wind speed and load resistance, which led to a rapid discharge of the battery.

The graphs show that the change in wind speed is accompanied by throws of the moment of the wind wheel, which are explained by the inertia of the rotating masses WPI and require increased attention to the design of its mechanical part. In the intervals of constancy of the wind speed the moment of the winder slightly exceeds the moment of the generator due to the presence of the moment of friction. The speed of the generator tracks the change in wind speed with delay, due to the moment of inertia of the rotating masses, and little depends on the values of load resistance. The oscillator current experiences significant fluctuations, which is explained as a change in resistance $r_L(t)$ and $r_{BL}(t)$, and the current of the battery i_{RB} (on Fig. 5, and the charging current is accepted as positive, and bit - negative). The battery charge is generally maintained at a sufficient level, except for the indicated case of voltage failure on the load, and in the range of 14 to 23 V due to low load impedance.

Power of the wind wheel $P_{WW} = \Omega \cdot M_{WW}$ (Fig. 5,b) has sharp fluctuations according to the change in wind speed. The power of the generator consists of the power of the load, the ballast resistance, the capacity of the battery and the power of the windings of the generator windings. Due to the inertia of the system, the power of the generator $P_G = \Omega \cdot M_G$ changes smoothly and ranges from 2,5 kW to 3,7 kW. Since the voltage on the combined bus is virtually unchanged, load capacity graph $P_L = u^2/r_L(t)$ practically accurately repeats the schedule of change in load resistance $r_L(t)$. Battery capacity $P_{RB} = u^2 \cdot q_{RB}$ during the charge has a positive sign, and during discharge it is negative, and energizes the load at the power shortage of the generator. On the marginal discharge current 20 A the battery comes out only at the moment $t = 13$ s. At this time, its power is 1,3 kW. On Fig. 5,b also illustrated are ballast load power schedules $P_{BL} = u^2/r_{BL}(t)$ and losses in the windings of the generator $P_{win} = r \cdot u^2/r_L$.

Conclusions.

1. The proposed functional scheme of the power supply system is based on WPI low power with a generator on permanent magnets provides a given voltage level on the assembly bus, and hence on the clamps of the load, with significant fluctuations in wind speed from 8,4 to 13,5 m/s (on 62%) and the random nature of the change in the resistance of the load of 1,0 to 2,2 Ohm (in 2,2 times), which corresponds to the fluctuation of the load power from 1,8 to 3,0 kW.
2. The obtained mathematical models adequately describe stationary and transitional regimes WPI.
3. The use of non-direct wind turbines greatly improves the overall and overall dimensions of the system and leads to cheaper prices.
4. The use of a buffer battery of sufficient capacity, permanently attached to the load, provides a more stable voltage WPI in the conditions of random oscillations of wind speed and load power.

REFERENCES

1. Yang Z., Chai Y. A survey of fault diagnosis for onshore grid-connected converter in wind energy conversion systems. *Renewable and Sustainable Energy Reviews*, Vol. 66, 1 December 2016, pp. 345-359.
2. Gan L.K., Echenique Subiabre, E.J.P. A realistic laboratory development of an isolated wind-battery system. *Renewable Energy*, 2019, pp. 645-656.
3. Merizalde Y., Hernández-Callejo L., Duque-Perez O., Alonso-Gómez V. Maintenance models applied to wind turbines. A comprehensive overview. *Energies*, Vol. 12, Issue 2, 11 January 2019.
4. Halko S.V. Technologies and means of transformation of renewable energy sources for private households: monograph / S.V. Halko, V.Y. Zharkov, A.V. Zharkov. – Melitopol: Lux, 2019. – 215 p.

5. Jon Twidell and Tony Weir. Power from the wind // Renewable Energy Resources. - London and New York: Taylor & Francis, 2006, pp. 263- 323.
6. Pat. 104467 UA. IPC F03D 7/06 (2006.01), F03D1/06. Low-power low-power wind turbine generator / V.Y. Zharkov, V.Y. Chornenkyi, B.S. Novakh, A.V. Zharkov.- №201400015. Published. 10.02.2016.- Bulletin. №3.
7. Pat. 116576 UA. IPC H02K21/00, H02K16/00. Electric generator of flat design / S.V. Halko, B.S. Novakh, A.V. Zharkov.- №201612745. Published. 25.05.2017.- Bulletin. №10.
8. Zharkov V.Y. Analysis of wind energy charge unit operation [Electronic resource] / V.Y. Zharkov, V.I. Zhorov, S.V. Zhorov. - Electronic. Text data: on-line // Scientific bulletin of Tavria State Agrotechnological University/ TSATU. - Melitopol, 2012. -Vol. 2, №1.
9. Boubzizi S., Abid H., El hajjaji A., Chaabane M. Comparative study of three types of controllers for DFIG in wind energy conversion system. *Protection and Control of Modern Power Systems*, Vol. 3, Issue 1, 1 December 2018.
10. Siniscalchi-Minna S., Bianchi F.D., De-Prada-Gil M., Ocampo-Martinez C. A wind farm control strategy for power reserve maximization. *Renewable Energy*, Vol. 131, February 2019, pp. 37-44.
11. Zharkov V.Y. Modern issues of household wind energy development / V.Y. Zharkov // Modern problems of energy supply systems of industrial and household objects: Proceedings of I Ukrainian scientific and technical conference.. (October 18-19 2012., Donetsk) / "DVNZ" DonNTU. - Donetsk, 2012. - p. 127-128.
12. Bi H., Wang P., Wang Z. Common grounded H-type bidirectional DC-DC converter with a wide voltage conversion ratio for a hybrid energy storage system. *Energies*, Vol. 11, Issue 2, February 2018.

13. Cetrini A., Cianetti F., Corradini M.L., Ippoliti G., Orlando G. On-line fatigue alleviation for wind turbines by a robust control approach. *International Journal of Electrical Power and Energy Systems*, Vol. 1, (9) 2019, pp. 384-394.
14. Njiri J.G., Beganovic N., Do M.H., Söffker D. Consideration of lifetime and fatigue load in wind turbine control. *Renewable Energy*, Vol 131, 2019, pp. 818-828.